

## Fast Dynamic Control Behavior of a Capacitor Supported Dynamic Voltage Restorer (DVR)

Narender Jatoth<sup>1</sup>, M. Praveen Kumar<sup>2</sup>

Department of Electrical Engineering, Ramappa Engineering College, Affiliated to JNTUH, Warangal-506001.

### ABSTRACT

Dynamic voltage restorers (DVRs) are the most popular Devices in industry to reduce the undesirable effect of voltage sags/swells to sensitive loads. The DVR is a series connected device whose function is to maintain sensitive loads voltage within the permissible range. This work provides us to find the optimal location and the optimal DVR settings to enhance the distribution related loading issues. It is based on the boundary control method with the second-order switching surface. The load voltage can ideally be reverted to the steady state in two switching actions during a supply voltage dip. The outer loop is used to generate the DVR output reference for the inner loop. It has three control modes for achieving two different functions, including the output regulation and output restoration. The first mode is for regulating the capacitor voltage on the dc side of the inverter, so that the output of the DVR is regulated at the nominal voltage. Conventional voltage-restoration technique is based on injecting voltage being in-phase with the supply voltage. The injected voltage magnitude will be the minimum, but the energy injected by the DVR is no minimal. In order to minimize the required capacity of the dc source, a minimum energy injection concept is taken into the considerations. It is based on maximizing the active power delivered by the supply mains and the reactive power handled by the DVR during the sag and swell cases. The review model has been built and tested the dynamic behaviors of the model under different sagged and swelled conditions and depths will be investigated. The quality of the load voltage under unbalanced and distorted phase voltages, and nonlinear inductive load is analyzed.

**Keywords** – Voltage sag, voltage swell, dynamic voltage restoration (DVR), power quality, fluctuation.

### I. INTRODUCTION

Reliability of supply and power quality (PQ) are two most important facets of any power delivery system today. Not so long ago, the main concern of consumers of electricity was the continuity of supply. However nowadays, consumers want not only continuity of supply, but

the quality of power is very important to them too. The power quality problems in distribution power systems are not new, but customer awareness of these problems has recently increased. The power quality at the point of common coupling (PCC) with the utility grid is governed by the various standards and the IEEE-519 standard is widely accepted.

Utilities and researchers all over the world have for decades worked on the improvement of power quality. There are sets of conventional solutions to the power quality problems, which have existed for a long time. However these conventional solutions use passive elements and do not always respond correctly as the nature of the power system conditions change. The increased power capabilities, ease of control, and reduced costs of modern semiconductor devices have made power electronic converters affordable in a large number of applications. New flexible solutions to many power quality problems have become possible with the aid of these power electronic converters.

Nowadays equipment made with semiconductor devices appears to be as sensitive and polluting as ever. Non-linear devices, such as power electronics converters, increase overall reactive power demanded by the equivalent load, and injects harmonic currents into the distribution grid. It is well known that the reactive power demand causes a drop in the feeder voltage and increases the losses. The presence of harmonic currents can cause additional losses and voltage waveform distortions, and so cause poor power quality. Also, the number of sensitive loads that require ideal sinusoidal supply voltages for their proper operation has increased. The increasing use of electronic equipment sensitive to power variations drives the interest in power conditioning technologies. So, in order to keep the power quality within limits proposed by standards, it is necessary to include some sort of compensation.

The power electronic based power conditioning devices can be effectively utilized to improve the quality of power supplied to customers. One modern solution that deals with both load current and supply voltage imperfections is the Unified Power Quality Conditioner (UPQC), which was first presented in 1995 by Hirofumi Akagi. Such a solution can compensate for different power

quality phenomena, such as: sags, swells, voltage imbalance, flicker, harmonics and reactive currents.

UPQC is a combination of series and shunt active filters connected in cascade via a common dc link capacitor. The series active filter inserts a voltage, which is added at the point of the common coupling (PCC) such that the load end-voltage remains unaffected by any voltage disturbance. The main objectives of the shunt active filter are: to compensate for the load reactive power demand and unbalance, to eliminate the harmonics from the supply current, and to regulate the common dc link voltage.

Dynamic voltage restorer (DVR) is presently one of the most cost-effective and thorough solutions to mitigate voltage sags by establishing proper quality voltage level for utility customers [3]. Its function is to inject a voltage in series with the supply and compensate for the difference between the nominal and sagged supply voltage. The injected voltage is typically provided by an inverter, which is powered by a dc source, such as batteries, flywheels, externally powered rectifiers, and capacitors.

Voltage restoration involves determining the amount of energy and the magnitude of the voltage injected by the DVR. Conventional voltage-restoration technique is based on injecting a voltage being in-phase with the supply voltage. The injected voltage magnitude will be the minimum, but the energy injected by the DVR is non minimal.

In order to minimize the required capacity of the dc source, a minimum energy injection (MEI) concept is proposed in. It is based on maximizing the active power delivered by the supply mains and the reactive power handled by the DVR during the sag. Determination of the injected-voltage magnitude is based on a real-time iterative method to minimize the active power injection by the DVR. This can then enhance the ride-through capability. However, the operation of each phase is individually controlled. There is no energy interaction between the un-sagged phase(s) and the sagged phase(s), in order to enhance the voltage restoration. Moreover, as the computation method is purely based on sinusoidal waveforms, the implementation is complicated in distribution network with nonlinear load. A sliding window over one line cycle of the fundamental frequency is proposed to determine the active and reactive power at the fundamental frequency. The lengthy computation time of the injected voltage phasor will cause output distortion after voltage sag.

Instead of using an external energy storage device, the methods are taking the active power for the inverter from the transmission system via a shunt-connected rectifier. The series inverter by itself has the capability to provide real-series

compensation to the line. The rectifier-based source requires a separate service supply, while the battery-based source requires regular maintenance and is not environment friendly. No external source is required in the DVR. The required phase and magnitude of the inverter load-voltage phasor are derived by considering the energy balance between the supply and the load, but the advantage is offset by the lengthy digital transformation and inversion of symmetrical components and calculation of the power consumption. The wave shape of the load voltage will be distorted and will take a relatively long settling time. As the supply voltage is assumed to be sinusoidal in the calculation, the load voltage will be affected and distorted with non sinusoidal supply voltage and load current. A single-phase capacitor-supported DVR can ideally revert the load voltage to steady state in two switching actions after voltage sags. By extending the concept, an analog-based three-phase capacitor-supported interline DVR is presented [19]–[21].

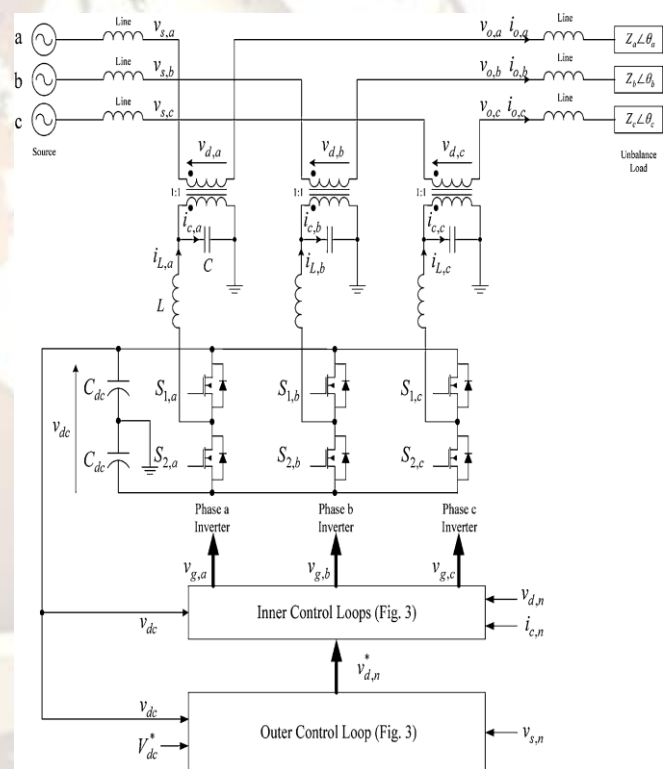


Fig.1. Proposed DVR structure

## HEADINGS

### 1. INTRODUCTION

### 2. DYNAMIC VOLTAGE RESTORER

#### 2.1. Introduction

##### 2.1.1. Voltage Source Converter

##### 2.1.2. Boost or Injection Transformers

##### 2.1.3. Passive Filters

##### 2.1.4. Energy Storage

#### 2.2. Control Strategy

##### 2.2.1. Pre-Sag Compensation

- 2.2.2. In-Phase Compensation
- 2.2.3. Minimum Energy Compensation
- 2.3. Control and Protection
- 2.4. Summary
- 3. INVERTER**
- 3.1. Introduction
  - 3.1.1. Basic Designs
  - 3.1.2. Total Harmonic Distortion
- 3.2. Single-Phase Voltage Source Inverter
  - 3.2.1. Types of VSI
- 3.3. Applications
- 3.4. Summary
- 4. MODELING OF DVR**
- 4.1. Principles of Operation
- 4.2. Review of Inner Loop
- 4.3. Characteristics of Outer Loop
- 4.4. Simplified Design Procedures
- 4.5 Results Analysis
  - 4.5.1. Harmonic Distortions
  - 4.5.2. Voltage Sag
  - 4.5.3. Voltage Swell
- 4.6. Comparison of results with and without DVR
- 5. CONCLUSION**
- 6. REFERENCES**

## **II. DYNAMIC VOLTAGE RESTORER**

### **2.1. INTRODUCTION**

The major objectives are to increase the capacity utilization of distribution feeders (by minimizing the rms values of the line currents for a specified power demand), reduce the losses and improve power quality at the load bus. The major assumption was to neglect the variations in the source voltages. This essentially implies that the dynamics of the source voltage is much slower than the load dynamics. When the fast variations in the source voltage cannot be ignored, these can affect the performance of critical loads such as (a) semiconductor fabrication plants (b) paper mills (c) food processing plants and (d) automotive assembly plants. The most common disturbances in the source voltages are the voltage sags or swells that can be due to

- i) Disturbances arising in the transmission system
- ii) Adjacent feeder faults and
- iii) Fuse or breaker operation.

Voltage sags of even 10% lasting for 5-10 cycles can result in costly damage in critical loads. The voltage sags can arise due to symmetrical or unsymmetrical faults. In the latter case, negative and zero sequence components are also present. Uncompensated nonlinear loads in the distribution system can cause harmonic components in the supply voltages. To mitigate the problems caused by poor quality of power supply, series connected compensators are used. These are called as Dynamic Voltage Restorer (DVR) in the literature as their primary application is to compensate for voltage

sags and swells. Their configuration is similar to that of SSSC. However, the control techniques are different. Also, a DVR is expected to respond fast (less than 1/4 cycle) and thus employs PWM converters using IGBT or IGCT devices. The first DVR entered commercial service on the Duke Power System in U.S.A. in August 1996. It has a rating of 2 MVA with 660 kJ of energy storage and is capable of compensating 50% voltage sag for a period of 0.5 second (30 cycles). It was installed to protect a highly automated yarn manufacturing and rug weaving facility. Since then, several DVRs have been installed to protect microprocessor fabrication plants, paper mills etc. Typically, DVRs are made of modular design with a module rating of 2 MVA or 5 MVA. They have been installed in substations of voltage rating from 11 kV to 69 kV. A DVR has to supply energy to the load during the voltage sags. If a DVR has to supply active power over longer periods, it is convenient to provide a shunt converter that is connected to the DVR on the DC side. As a matter of fact one could envisage a combination of DSTATCOM and DVR connected on the DC side to compensate for both load and supply voltage variations. In this section, we discuss the application of DVR for fundamental frequency voltage. The voltage source converter is typically one or more converters connected in series to provide the required voltage rating. The DVR can inject a (fundamental frequency) voltage in each phase of required magnitude and phase. The DVR has two operating modes

- A. Standby (also termed as short circuit operation (SCO) mode) where the voltage injected has zero magnitude.
- B. Boost (when the DVR injects a required voltage of appropriate magnitude and phase to restore the prefault load bus voltage).

The power circuit of DVR shown in Fig.

2.1 has four components listed below

#### 2.1.1. Voltage Source Converter (VSC):

This could be a 3 phase - 3 wire VSC or 3 phase - 4 wire VSC. The latter permits the injection of zero-sequence voltages. Either a conventional two level converter (Graetz bridge) or a three level converter is used.

#### 2.1.2. Boost or Injection Transformers:

Three single phase transformers are connected in series with the distribution feeder to couple the VSC (at the lower voltage level) to the higher distribution voltage level. The three single transformers can be connected with star/open star winding or delta/open star winding. The latter does not permit the injection of the zero sequence voltage. The choice of the injection transformer winding depends on the connections of the step down transformer that feeds the load. If ac Y connected transformer (as shown in Fig. 2.1) is used, there is no need to compensate the zero

sequence voltages. However if Y|Y connection with neutral grounding is used, the zero sequence voltage may have to be compensated. It is essential to avoid the saturation in the injection transformers.

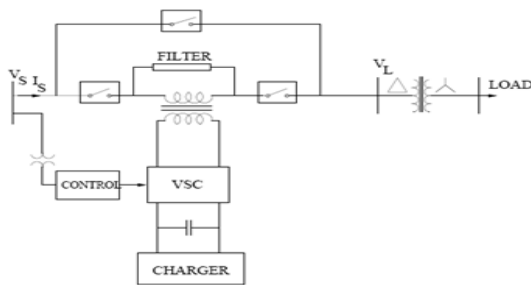


Fig. 2.1 Power circuit of DVR

### 2.1.3. Passive Filters:

The passive filters can be placed either on the high voltage side or the converter side of the boost transformers. The advantages of the converter side filters are (a) the components are rated at lower voltage and (b) higher order harmonic currents (due to the VSC) do not flow through the transformer windings. The disadvantages are that the filter inductor causes voltage drop and phase (angle) shift in the (fundamental component of) voltage injected. This can affect the control scheme of DVR. The location of the filter on the high voltage side overcomes the drawbacks (the leakage reactance of the transformer can be used as a filter inductor), but results in higher ratings of the transformers as high frequency currents can flow through the windings.

### 2.1.4. Energy Storage:

This is required to provide active power to the load during deep voltage sags. Lead-acid batteries, flywheel or SMES can be used for energy storage. It is also possible to provide the required power on the DC side of the VSC by an auxiliary bridge converter that is fed from an auxiliary AC supply.

## 2.2. CONTROL STRATEGY

There are three basic control strategies as follows:

### 2.2.1. Pre-Sag Compensation:

The supply voltage is continuously tracked and the load voltage is compensated to the pre-sag condition. This method results in (nearly) undisturbed load voltage, but requires higher rating of the DVR. Before a sag occur,  $V_s = V_L = V_o$ . The voltage sag results in drop in the magnitude of the supply voltage to  $V_{s1}$ . The phase angle of the supply also may shift see Fig. 2.2. The DVR injects a voltage  $V_{C1}$  such that the load voltage ( $V_L = V_{s1} + V_{C1}$ ) remains at  $V_o$  (both in magnitude and phase). It is claimed that some loads are sensitive to phase

jumps and it is necessary to compensate for both the phase jumps and the voltage sags.

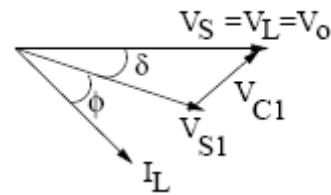


Fig. 2.2 Pre-Sag Compensation Phasor diagram

### 2.2.2. In-phase Compensation:

The voltage injected by the DVR is always in phase with the supply voltage regardless of the load current and the pre-sag voltage ( $V_o$ ). This control strategy results in the minimum value of the injected voltage (magnitude). However, the phase of the load voltage is disturbed. For loads which are not sensitive to the phase jumps, this control strategy results in optimum utilization of the voltage rating of the DVR. The power requirements for the DVR are not zero for these strategies.

### 2.2.3. Minimum Energy Compensation:

Neglecting losses, the power requirements of the DVR are zero if the injected voltage ( $V_C$ ) is in quadrature with the load current. To raise the voltage at the load bus, the voltage injected by the DVR is capacitive and  $V_L$  leads  $V_{s1}$  (see Fig. 2.3). Fig. 2.3 also shows the in-phase compensation for comparison. It is to be noted that the current phasor is determined by the load bus voltage phasor and the power factor of the load.

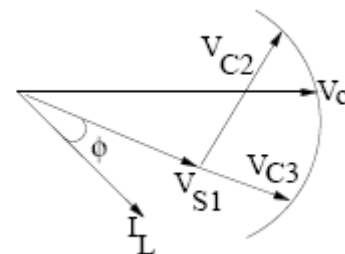


Fig. 2.3 Minimum Energy Compensation Phasor diagram

Implementation of the minimum energy compensation requires the measurement of the load current phasor in addition to the supply voltage. When  $V_C$  is in quadrature with the load current, DVR supplies only reactive power. However, full load voltage compensation is not possible Unless the supply voltage is above a minimum value that depends on the load power factor. When the magnitude of  $V_C$  is not constrained, the minimum value of  $V_s$  that still allows full compensation is where  $\phi$  is the power factor angle and  $V_o$  is the required magnitude of the Load bus voltage. If the magnitude of the injected voltage is limited ( $V_{max C}$ ), the minimum supply voltage that allows full compensation is given by the expressions figures

(2.1) and (2.2). Note that at the minimum source voltage, the current is in phase with  $V_s$  for the case (a).

### 2.3. CONTROL AND PROTECTION

The control and protection of a DVR designed to compensate voltage sags must consider the following functional requirements.

1. When the supply voltage is normal, the DVR operates in a standby mode with zero voltage injection. However if the energy storage device (say batteries) is to be charged, then the DVR can operate in a self- charging control mode.

2. When a voltage sag/swell occurs, the DVR needs to inject three single phase voltages in synchronism with the supply in a very short time. Each phase of the injected voltage can be controlled independently in magnitude and phase. However, zero sequence voltage can be eliminated in situations where it has no effect. The DVR draws active power from the energy source and supplies this along with the reactive power (required) to the load.

3. If there is a fault on the downstream of the DVR, the converter is by- passed temporarily using thyristor switches to protect the DVR against over currents. The threshold is determined by the current ratings of the DVR.

The overall design of DVR must consider the following parameters:

1. Ratings of the load and power factor
2. Voltage rating of the distribution line
3. Maximum single phase sag (in percentage)
4. Maximum three phase sag (in percentage)
5. Duration of the voltage sag (in milliseconds)
6. The voltage time area (this is an indication of the energy requirements)
7. Recovery time for the DC link voltage to 100%

Typically, a DVR may be designed to protect a sensitive load against 35% of three phase voltage sags or 50% of the single phase sag. The duration of the sag could be 200 ms. The DVR can compensate higher voltage sags lasting for shorter durations or allow longer durations up to 500 ms for smaller voltage sags. The response time could be as small as 1 ms.

### 2.4. SUMMARY:

DVR is used in the power system network mainly to mitigate the power quality issues related to voltage sags and voltage swells. It contains fast dynamic switching devices like IGBT to facilitate fast switching action and has a frequency of 10 KHz. The voltage source inverters converts AC to DC supply to charge the capacitor banks when a swell occurs and converts DC to AC supply and injects a voltage in series with the line to overcome the effect of voltage sag. The components used in the DVR model are  $V_{sc}$ , boosting transformer,

passive filters to overcome the harmonics which while switching the IGBTs. To reduce the cost required by the storage devices we can opt for a closed loop control to charge the capacitor banks from the supply itself irrespective of sagged or swelled conditions.

## III. INVERTER

### 3.1. INTRODUCTION

The main objective of static power converters is to produce an ac output waveform from a dc power supply. These are the types of waveforms required in adjustable speed drives (ASDs), uninterruptible power supplies (UPS), static var compensators, active filters, flexible ac transmission systems (FACTS), and voltage compensators, which are only a few applications. For sinusoidal ac outputs, the magnitude, frequency, and phase should be controllable. According to the type of ac output waveform, these topologies can be considered as voltage source inverters (VSIs), where the independently controlled ac output is a voltage waveform.

These structures are the most widely used because they naturally behave as voltage sources as required by many industrial applications, such as adjustable speed drives (ASDs), which are the most popular application of inverters; see Fig 3.1. Similarly, these topologies can be found as current source inverters (CSIs), where the independently controlled ac output is a current waveform. These structures are still widely used in medium-voltage industrial applications, where high-quality voltage waveforms are required. Static power converters, specifically inverters, are constructed from power switches and the ac output waveforms are therefore made up of discrete values. This leads to the generation of waveforms that feature fast transitions rather than smooth ones. For instance, the ac output voltage produced by the VSI of a standard ASD is a three-level

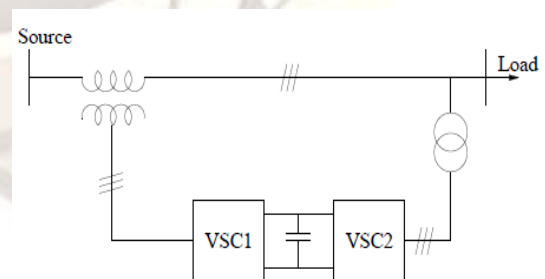


Fig 3.1 Inverter DC link

#### 3.1.1. Basic designs:

In one simple inverter circuit, DC power is connected to a transformer through the centre tap of the primary winding. A switch is rapidly switched back and forth to allow current to flow back to the DC source following two alternate paths through

one end of the primary winding and then the other. The alternation of the direction of current in the primary winding of the transformer produces alternating current (AC) in the secondary circuit. The electromechanical version of the switching device includes two stationary contacts and a spring supported moving contact. The spring holds the movable contact against one of the stationary contacts and an electromagnet pulls the movable contact to the opposite stationary contact. The current in the electromagnet is interrupted by the action of the switch so that the switch continually switches rapidly back and forth. This type of electromechanical inverter switch, called a vibrator or buzzer, was once used in vacuum tube automobile radios. A similar mechanism has been used in door bells, buzzers and tattoo. As they became available with adequate power ratings, transistors and various other types of semiconductor switches have been incorporated into inverter circuit designs.

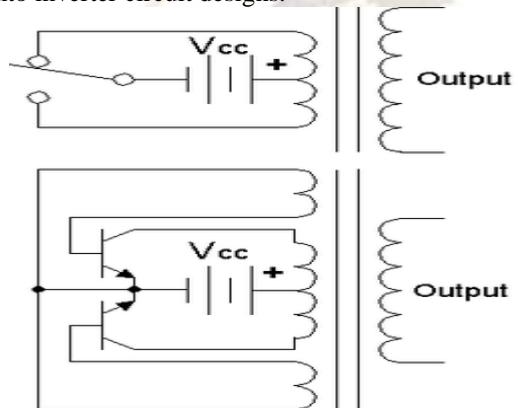


Fig 3.2 switching of MOSFET

The switch in the simple inverter described above, when not coupled to an output transformer, produces a square voltage waveform due to its simple off and on nature as opposed to the sinusoidal waveform that is the usual waveform of an AC power supply. Using Fourier analysis, periodic waveforms are represented as the sum of an infinite series of sine waves. The sine wave that has the same frequency as the original waveform is called the fundamental component. The other sine waves, called harmonics, which are included in the series have frequencies that are integral multiples of the fundamental frequency. The quality of the inverter output waveform can be expressed by using the Fourier analysis data to calculate the total harmonic distortion (THD) Fig3.3. The total harmonic distortion is the square root of the sum of the squares of the harmonic voltages divided by the fundamental voltage:

$$THD = \frac{\sqrt{v_2^2 + v_3^2 + v_4^2 + \dots + v_n^2}}{v_1} \quad \dots 3.1$$

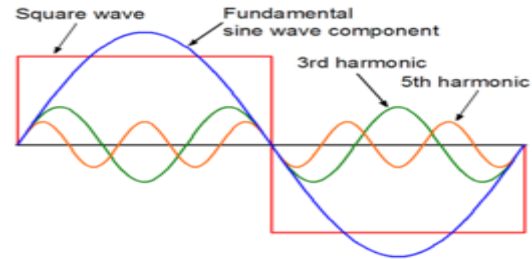


Fig 3.3 Total harmonic distortion

### 3.2. Single-Phase Voltage Source Inverter:

Single-phase voltage source inverters (VSI's) can be found as half-bridge and full-bridge topologies. Although the power range they cover is the low one, they are widely used in power supplies, single-phase UPS's, and currently to form elaborate high-power static power topologies, such as for instance, the multi cell configurations that are reviewed. The main features of both approaches are reviewed and presented in the following.

#### 3.2.1. Types of VSI:

##### A. Half-Bridge VSI

The power topology of a half-bridge VSI, where two large capacitors are required to provide a neutral point N, such that each capacitor maintains a constant voltage= $V_i/2$ . Because the current harmonics injected by the operation of the inverter are low-order harmonics, a set of large capacitors ( $C_+$  and  $C_-$ ) is required. It is clear that both switches  $S_+$  and  $S_-$  cannot be on simultaneously because short circuit across the dc link voltage source  $V_i$  would be produced. In order to avoid the short circuit across the DC bus and the undefined ac output voltage condition, the modulating technique should always ensure that at any instant either the top or the bottom switch of the inverter leg is on.

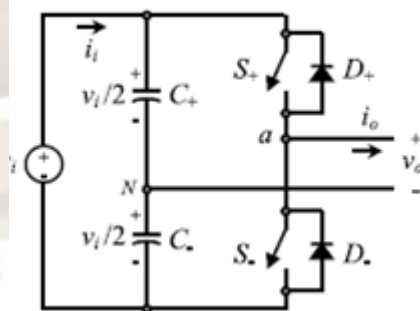


Fig 3.4 Half-bridge inverter

shows the ideal waveforms associated with the half-bridge inverter shown in Fig 3.4. The states for the switches  $S_+$  and  $S_-$  are defined by the modulating technique, which in this case is a carrier-based PWM. The Carrier-Based Pulse width Modulation (PWM) Technique: As mentioned earlier, it is desired that the ac output voltage.  $V_{a,N}$  follow a

given waveform (e.g., sinusoidal) on a continuous basis by properly switching the power valves. The carrier-based PWM technique fulfils such a requirement as it defines the on and off states of the switches of one leg of a VSI by comparing a modulating signal  $V_c$  (desired ac output voltage) and a triangular waveform  $V_d$  (carrier signal). In practice, when  $V_c > V_d$  the switch  $S_1$  is on and the switch  $S_2$  is off; similarly, when  $V_c < V_d$  the switch  $S_1$  is off and the switch  $S_2$  is on. A special case is when the modulating signal  $V_c$  is a sinusoidal at frequency  $f_c$  and amplitude  $V_{c1}$ , and the triangular signal  $V_d$  is at frequency  $f_D$  and amplitude  $V_d$ . This is the sinusoidal PWM (SPWM) scheme. In this case, the modulation index  $m_a$  (also known as the amplitude-modulation ratio) is defined as

$$m_a = \frac{v_{c1}}{v_A} \quad \dots 3.2$$

And the normalized carrier frequency  $m_f$  (also known as the frequency-modulation ratio) is

$$m_f = \frac{f_D}{f_c} \quad \dots 3.3$$

$v_{a1}$  is basically a sinusoidal waveform plus harmonics, which features: (a) the amplitude of the fundamental component of the ac output voltage  $v_{o1}$  satisfying the following expression:

$$v_{o1} = v_{a1} = \frac{v_i}{2} m_a \quad \dots 3.4$$

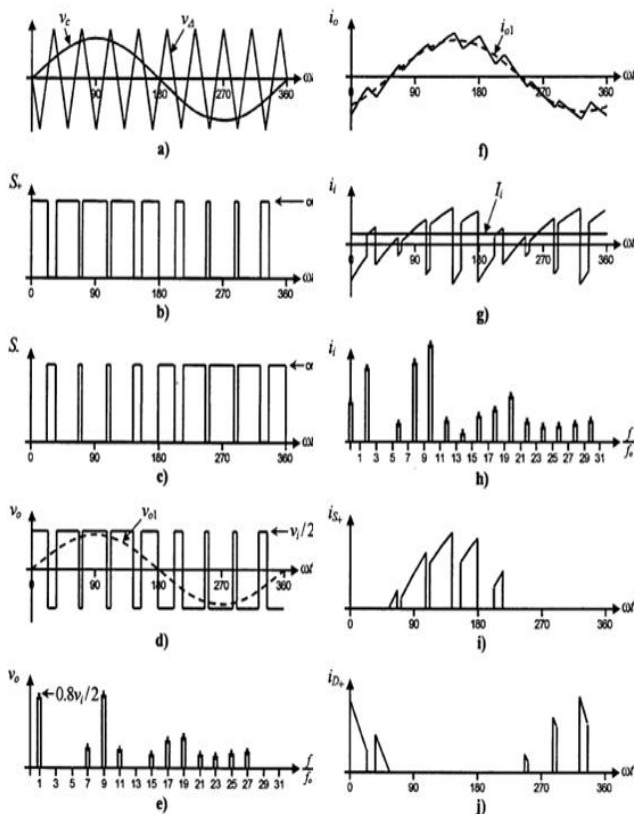


Fig 3.5. Pulse width modulation

will be discussed later); (b) for odd values of the normalized carrier frequency of the harmonics in the ac output voltage appear at normalized frequencies  $f_h$  centered around  $m_f$  and its multiples, specifically,

$$h = lm_f \pm k \quad \text{where } l=1,2,3 \quad \dots \dots 3.5$$

Where  $k=2; 4; 6; \dots$  for  $l=1; 3; 5; \dots$ ; and  $k=1; 3; 5; \dots$  for  $l=2; 4; 6; \dots$ ; (c) the amplitude of the ac output voltage harmonics is a function of the modulation index  $m_a$  and is independent of the normalized carrier frequency  $m_f$  for  $f > 9$ ; (d) the harmonics in the dc link current (due to the modulation) appear at normalized frequencies  $f_p$  centered around the normalized carrier frequency  $m_f$  and its multiples, specifically,

$$h = lm_f \pm k \pm 1 \quad \text{where } l=1,2,3.. \quad \dots 3.6$$

Where  $k=2; 4; 6; \dots$  for  $l=1; 3; 5; \dots$ ; and  $k=1; 3; 5; \dots$  for  $l=2; 4; 6; \dots$ . Additional important issues are: (a) for small values of  $m_f$  ( $m_f < 21$ ), the carrier signal  $V_d$  and the modulating signal  $V_c$  should be synchronized to each other ( $m_f$  integer), which is required to hold the previous features; if this is not the case, sub harmonics will be present in the ac output voltage; (b) for large values of  $m_f$  ( $m_f > 21$ ), the sub harmonics are negligible if an asynchronous PWM technique is used, however, due to potential very low-order sub harmonics, its use should be avoided;

Inverters

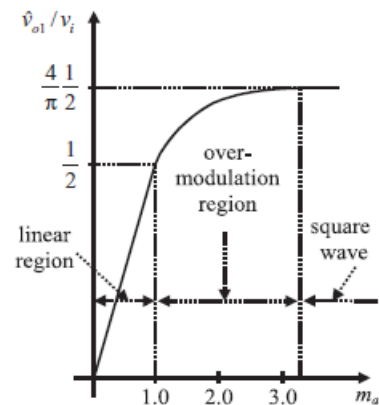


Fig.3.6. Modulation region

finally (c) in the over modulation region ( $m_a > 1$ ) some intersections between the carrier and the modulating signal are missed, which leads to the generation of low-order harmonics but a higher fundamental ac output voltage is obtained; unfortunately, the linearity between  $m_a$  and  $v_{o1}$  achieved in the linear region does not hold in the over modulation region, moreover, a saturation effect can be observed.

The PWM technique allows an ac output voltage to be generated that tracks a given modulating signal. A special case is the SPWM technique (the modulating signal is a sinusoidal) that provides in the linear region an ac output voltage that varies linearly as a function of the modulation

index and the harmonics are at well-defined frequencies and amplitudes.

These features simplify the design of filtering components. Unfortunately, the maximum amplitude of the fundamental ac voltage is  $V_i/2$  in this operating mode. Higher voltages are obtained by using the over modulation region ( $m_a > 1$ ); however, low-order harmonics appear in the ac output voltage.

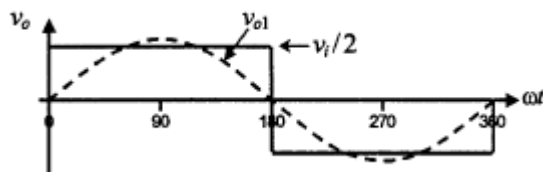


Fig3.7 Voltage wave forms

### B. Square-Wave Modulating Technique:

Both switches  $S_x$  and  $S_{\bar{x}}$  are on for one-half cycle of the AC output period. This is equivalent to the SPWM technique with an infinite modulation index  $m_a$ . Figure 3.5 shows the following: (a) the normalized AC output voltage harmonics are at frequencies  $h = 3; 5; 7; 9; \dots$ , and for a given DC link voltage; (b) the fundamental ac output voltage features an amplitude given by

$$v_{o1} = v_{aN1} = \frac{4 v_i}{\pi 2} \quad \dots 3.7$$

and the harmonics feature an amplitude given by equation (3.8)

$$v_{oh} = \frac{v_{o1}}{h} \quad \dots 3.8$$

### C. Full-Bridge VSI:

The power topology of a full-bridge VSI. This inverter is similar to the half-bridge inverter; however, a second leg provides the neutral point to the load. As expected, both switches  $S_1$  and  $S_{1\bar{}}$  (or  $S_2$  and  $S_{2\bar{}}$ ) cannot be on simultaneously because a short circuit across the dc link voltage source  $v_i$  would be produced. The undefined condition should be avoided so as to be always capable of defining the ac output voltage. In order to avoid the short circuit across the dc bus and the undefined ac output voltage condition, the modulating technique should ensure that either the top or the bottom switch of each leg is on at any instant. It can be observed that the ac output voltage can take values up to the dc link value  $v_i$  which is twice that obtained with half-bridge VSI topologies.

Several modulating techniques have been developed that are applicable to full-bridge VSIs. Among them are the PWM (bipolar and unipolar) techniques.

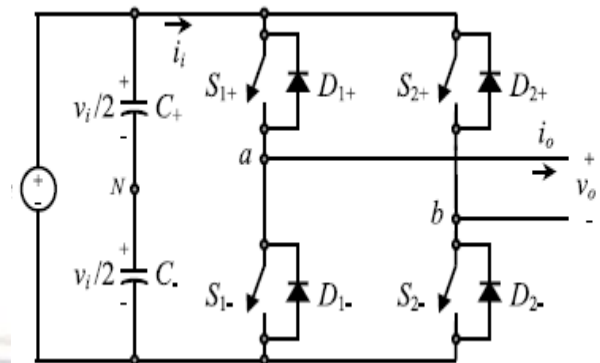


Fig 3.8 Full-bridge inverter

### D. Bipolar PWM Technique:

States 1 and 2 are used to generate the ac output voltage in this approach. Thus, the ac output voltage waveform features only two values, which are  $V_i$  and  $-V_i$ . To generate the states, a carrier-based technique can be used a sine half-bridge configurations where only one sinusoidal modulating signal has been used. It should be noted that the on state in switch  $S_x$  in the half-bridge corresponds to both switches  $S_{1x}$  and  $S_{2\bar{x}}$  being in the on state in the full-bridge configuration. Similarly,  $S_{\bar{x}}$  in the on state in the half-bridge corresponds to both switches  $S_{1\bar{x}}$  and  $S_{2x}$  being in the on state in the full-bridge configuration. This is called bipolar carrier-based SPWM. The ac output voltage waveform in a full-bridge VSI is basically a sinusoidal waveform that features a fundamental component of amplitude  $v_{o1}$  that satisfies the expression

$$v_{o1} = v_{ab1} = (v_i \times m_a) \quad \dots 3.9$$

In the linear region of the modulating technique ( $m_a \leq 1$ ), which is twice that obtained in the half-bridge VSI. Identical conclusions can be drawn for the frequencies and amplitudes of the harmonics in the ac output voltage and dc link current, and for operations at smaller and larger values of odd  $m_f$  (including the over modulation region ( $m_a > 1$ )), than in half bridge VSIs, but considering that the maximum ac output voltage is the DC link voltage  $v_i$ .

Thus, in the over modulation region the fundamental component of amplitude  $V_{O1}$  satisfies the expression

$$v_i < v_{o1} = v_{ab} < \frac{4}{\pi} v_i \quad \dots 3.10$$

In contrast to the bipolar approach, the unipolar PWM technique uses the states 1, 2, 3, and to generate the ac output voltage. Thus, the ac output voltage waveform can instantaneously take one of three values, namely  $v_i, -v_i$ . The signal  $u_c$  is used to

generate  $v_{an}$ , and  $-U_c$  is used to generate  $U_{bN}$ ;  $-U_{bN1} = U_{aN1}$ . On the other hand,

$$v_{o1} = v_{aN1} - v_{bN1} = (2 \times v_{aN1}) \text{ thus}$$

$$v_{o1} = (2 \times v_{aN1}) = (m_a \times v_{aN1})$$

This is called unipolar carrier-based PWM. Identical conclusions can be drawn for the amplitude of the fundamental component and harmonics in the ac output voltage and dc link current, and for operations at smaller and larger values of  $m_f$ , (including the over modulation region ( $m_a > 1$ )), than in full-bridge VSIs modulated by the bipolar SPWM. However, because the phase voltages  $U_{aN}$  and  $U_{bN}$  are identical but 180 out of phase, the output voltage

$U_o = U_{aN} - U_{bN} = U_{ab}$  will not contain even harmonics. Thus, if  $m_f$  is taken even, the harmonics in the ac output voltage appear at normalized odd frequencies  $h$  centered around twice the normalized carrier frequency  $m_f$  and its multiples. Specifically,

$$h = lm_f \pm k \text{ where } l=2,4,\dots \text{ Where } k=1,3,5,\dots$$

and the harmonics in the dc link current appear at normalized frequencies  $f_p$  centered around twice the normalized carrier frequency  $m_f$  and its multiples. Specifically,  $h = lm_f \pm k \pm 1$  where  $l=2,4,\dots$

Where  $k=1,3,5,\dots$  This feature is considered to be an advantage because it allows the use of smaller filtering components to obtain high quality voltage and current waveforms while using the same switching frequency as in VSIs modulated by the bipolar approach.

### 3.3. APPLICATIONS

The various applications of voltage source inverter are as follows

1. DC power source utilization
  2. Uninterruptible power supplies
  3. HVDC power transmission & Variable-frequency drives
  4. Electric vehicle drives
  5. Air conditioning
- 3.4. SUMMARY

The voltage source converter consists of IGBT switches to provide high speed switching actions as they operate for higher frequency around 10 KHz. The voltage source inverter converts AC to DC supply to charge the capacitor banks when a swell occurs and converts DC to AC supply and injects a voltage in series with the line to overcome the effect of voltage sag. The pulse width modulation technique is used to generate the firing pulses to turn on the IGBTs in half bridge and full bridge configurations.

## IV. MODELING OF DVR

### 4.1. PRINCIPLES OF OPERATION

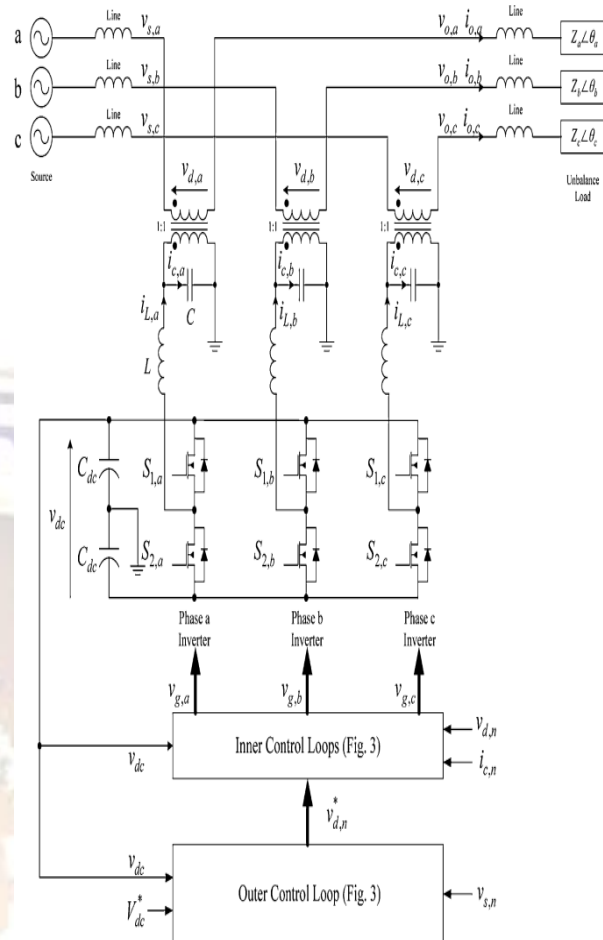


Fig. 4.1. Structure of the proposed interlines DVR and its connection to the utility.

Fig. 4.1 shows the circuit schematic of the DVR with three phase transmission system. It consists of inverters, output LC filters, and injection transformers. The dc side is connected to a capacitor bank, formed by two capacitors. Each capacitor has the value of  $C_{dc}$ . The inverter shown in Fig. 4.1 is a half bridge configuration. However, the operation is similar in the full bridge configuration. The DVR is operated as a controllable voltage source  $v_{d,n}$ , where  $n$  represents either phase a, b, or c. It is connected between the supply and the load. The relationship among the supply voltage  $v_{s,n}$ , the load voltage  $v_{d,n}$  and  $v_{o1}$ .

$$v_{d,n}(t) = v_{s,n}(t) - v_{o,n}(t) \quad \dots 4.1$$

Fig. 4.3 shows the phasor diagrams of  $v_{s,m}$ ,  $v_{o,m}$ ,  $v_{d,m}$ , and the load current  $i_{o,n}$  in voltage sag and unbalanced conditions. Fig. 4.2 shows the control block diagram of proposed control scheme. The control scheme consists of two main loops. The first control loop, namely inner loop, is formed in

each phase. It is used to generate the gate signals for the switches in the inverter, so that

$v_{d,n}^*$  will follow the DVR output reference  $v_{d,n}^*$ . This loop has fast dynamic response to external disturbances. Its operating principle is based on extending the boundary control technique with second-order switching surface in [19]–[21]. The second loop, namely outer loop, is used to generate  $v_{d,n}^*$ . Based on (Eq. 4.1)

$$v_{d,n}^*(t) = v_{s,n}(t) - v_{o,n}^*(t) \quad \dots 4.2$$

Where  $v_{o,n}^*$  is the load-voltage reference and is generated by the phase-lock loop (PLL)

The outer loop is used to regulate the dc-link voltage by adjusting the phase of the inverter load voltage with respect to the load current. Its bandwidth is set much lower than the line frequency. The purpose is to attenuate the undesirable signals, which are due to the ac component on the dc-link voltage and the load current, getting into the loop. Since the inner and outer loops have different dynamic behaviors, the controller will react differently in the voltage sags of short [22]–[25] and long durations. If the duration of the voltage sag is short, typically less than 0.5 s, the inner loop will react immediately and maintain the wave shape of the load voltage. The outer loop is relatively inert during the period. The sagged phase(s) will be supported purely by the capacitor bank. The capacitor voltage will decrease. After the voltage sag, the outer loop will start reacting to the decrease in the capacitor voltage. The capacitor will be charged up from the supply by adjusting the phase angle of the inverter output. If the duration of the voltage sag is long, the inner loop will keep the wave shape of the load voltage and the outer loop will regulate the dc-link voltage. Thus, the sagged phase(s) will be supported by the dc link, while electric energy will also be extracted from the un sagged phase(s) through the dc link. In the steady-state operation, as the frequency response of the inner loop is very fast, the wave shape of the load voltage can be kept sinusoidal, even if there are harmonic distortions in the supply voltage and the load current. Moreover, with the interline energy flow in the outer-loop control; the output quality can be maintained, even if there is an unbalanced supply voltage. At any time, the amplitude of  $v_{o,n}^*$  is fixed because the load voltage is regulated at the nominal value.  $v_{o,n}^*$  Has the same frequency as  $v_{s,n}$ , and the phase angle  $\beta$  between  $v_{o,n}^*$  and  $v_{s,n}$  is controlled by the signal  $v_{\beta}$  shown in Fig. 4.3. The supply voltages can be expressed as follows:

$$v_{s,a}(t) = v_{sm,a} \cos \omega t \quad \dots 4.3$$

$$v_{s,b}(t) = v_{sm,b} \cos(\omega t - 120) \quad \dots 4.4$$

$$v_{s,c}(t) = v_{sm,c} \cos(\omega t + 120) \quad \dots 4.5$$

Where  $V_{sm,a}$ ,  $V_{sm,b}$ , and  $V_{sm,c}$  are the peak values of the supply voltages of the phases a, b, and c, respectively, and  $\omega$  is the angular line frequency.

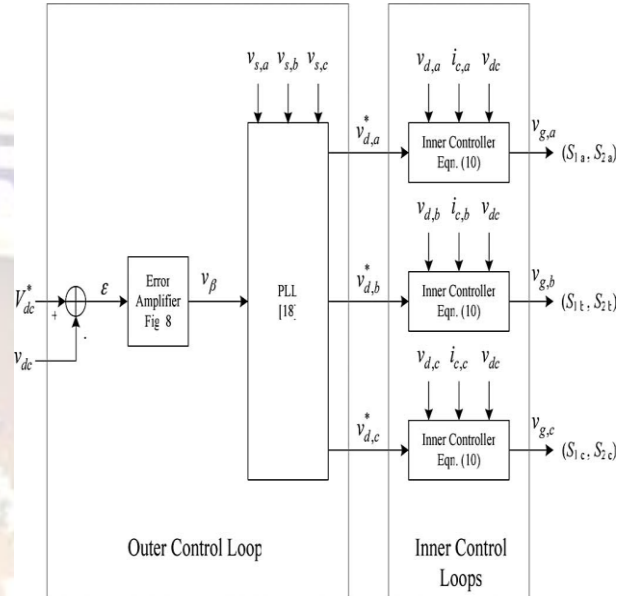


Fig.4.2 Block diagram of the proposed controller

#### 4.2. REVIEW OF INNER LOOP

The inner-loop control strategy is by using boundary control with second order switching surface [19]. A brief review of the inner loop will be given in this section. In one leg of the three-phase half-bridge inverter, which is shown in Fig. 4.1, as S1,n and S2,n are operated in anti phase and the output inductor current is continuous, two possible switching modes are derived, and their state-space equations are shown as follows.

When S1,n is OFF and S2,n is ON

$$\dot{x}_n = \begin{bmatrix} 0 & -1/L \\ 1/C & (-\frac{1}{R}) * C \end{bmatrix} x_n + \begin{bmatrix} -\frac{1}{2}L & 0 \\ 0 & (\frac{1}{R}) * C \end{bmatrix} u_n \quad \dots 4.6$$

$$u_{d,n} = [0 \quad 1] x_n \quad \dots 4.7$$

When S1,n is ON and S2,n is OFF

$$\dot{x}_n = \begin{bmatrix} 0 & -1/L \\ 1/C & (-\frac{1}{R}) * C \end{bmatrix} x_n + \begin{bmatrix} \frac{1}{2}L & 0 \\ 0 & (\frac{1}{R}) * C \end{bmatrix} u_n \quad \dots 4.8$$

$$u_{d,n} = \begin{bmatrix} 0 & 1 \end{bmatrix} x_n \quad \dots 4.9$$

$$\text{Where } k = L/2C \quad 4.15$$

$$\text{Where } x_n = [ i_{L,n} \ u_{C,n} ]^T ; u_n = [ V_{dc} \ V_{s,n} ]^T \dots 4.10$$

And  $R_{L,n}$  is the fictitious resistance showing the ratio between the load voltage and load current. Fig. 4.4(a) and (b) shows the equivalent circuits of the two modes corresponding to Eq. 4.6 to 4.10.

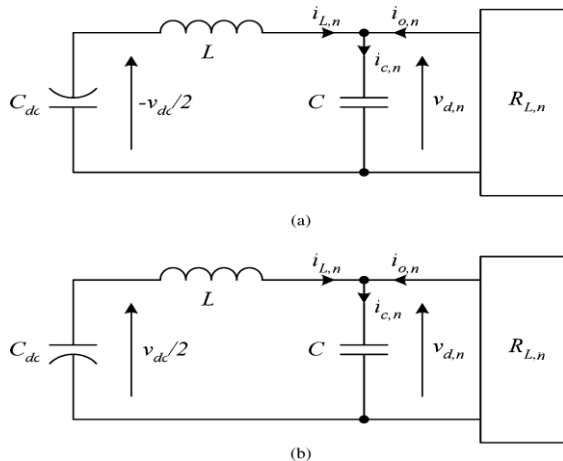


Fig.4.4. Equivalent circuits of one phase in the inverter system.

(a) S1,n is OFF and S2,n is ON (b) S1,n is ON and S2,n is OFF

**A. Criteria for Switching S1,n OFF and S2,n ON:**

S1,n and S2,n are originally ON and OFF, respectively [19]. S1,n and S2,n are going to switch OFF and ON, respectively. The criteria for switching S1,n OFF and S2,n ON are as follows:

$$u_{d,n}(t_1) \geq u_{d,n,max} - \frac{L}{2C} [ 1 / (U_{DC}(t_1)/2) + u_{d,n}(t_1) ]$$

$$i_{C,n}^2(t_1) \quad \dots 4.11$$

$$i_{C,n}(t_1) \geq 0$$

...4.12

**B. Criteria for Switching S1,n ON and S2,n OFF:**

S1,n and S2,n are originally OFF and ON, respectively. S1,n and S2,n are going to switch ON and OFF, respectively [19]. The criteria for switching S1,n ON and S2,n OFF are as follows:

$$u_{d,n}(t_3) \leq u_{d,n,min} + \frac{L}{2C} [ 1 / (U_{DC}(t_3)/2) - u_{d,n}(t_3) ]$$

$$i_{C,n}^2(t_3) \quad \dots 4.13$$

$$i_{C,n}(t_3) \leq 0 \quad \dots 4.14$$

Based on Eq.(8.6)–(8.9) and  $u_{d,n,min} = u_{d,n,max} = U_{d,n}^*$ , the general form of  $\sigma^2$  is defined as follows:

$$\sigma^2 [ i_{L,n}(t), u_{d,n}(t) ] = \frac{1}{k} [ u_{d,n}(t) - U_{d,n}^*(t) ] * [ \frac{v(t)}{2} + [ \text{sgn}[i_{C,n}(t)] u_{d,n}(t) ] + \text{sgn}[i_{C,n}(t)] i_{C,n}^2(t) ]$$

**4.3. CHARACTERISTICS OF OUTER LOOP**

**A. Steady-State Characteristics**

The function of the outer loop is to regulate  $U_{dc}$  at the reference value of  $U_{dc}^*$ . By applying the conservation of energy, the DVR will ideally have zero-average real power flow at the steady state.

$$P_{s,a} + P_{s,b} + P_{s,c} = P_{o,a} + P_{o,b} + P_{o,c} \quad \dots 4.16$$

$$P_a = P_b = P_c = 0 \quad \dots 4.17$$

$$P_{s,n} = U_{s,n} i_{o,n} \cos(\theta_n - \beta) \quad \dots 4.18$$

$$P_{o,n} = U_{o,n} i_{o,n} \cos(\theta_n) ; P_n = U_{d,n} i_{o,n} \cos(\phi_n) \quad \dots 4.19$$

where  $P_{s,n}$ ,  $P_{o,n}$ , and  $P_n$  are the input, output powers, and power transferred of the each phase, respectively,  $i_{o,n}$  is the load current of each phase,  $\theta_n$  is the phase angle between  $v_{o,n}$  and  $i_{o,n}$ ,  $\beta$  is the phase angle between  $v_{s,n}$  and  $v_{o,n}$ , and  $\phi_n$  is the phase angle between  $v_{d,n}$  and  $i_{o,n}$ . Under supply-voltage interruption, the outer loop will adjust the value of  $\beta$ . The DVR will generate the required magnitude and phase of  $v_{d,n}$  in each phase individually. The DVR will then absorb (deliver) electric energy from (to) the dc link. As the adjustment of  $\beta$  is common to the three phases, the sagged phase(s) will be supported by the capacitor bank and the un-sagged phase(s). The corresponding equations of  $v_{o,n}$  are as follows:

$$u_{o,a}(t) = V_{om,a} \cos(\omega t - \beta) \quad \dots 4.20$$

$$u_{o,b}(t) = V_{om,b} \cos(\omega t - 120^\circ - \beta) \quad \dots 4.21$$

$$u_{o,c}(t) = V_{om,c} \cos(\omega t + 120^\circ - \beta) \quad \dots 4.22$$

Where  $V_{om,n}$  is the peak load voltage of phase n.

Fig. 4.3 shows the steady-state phasor diagrams with one-phase sagged and three-phase voltage balancing, respectively. The parameters used are based on Tables 4.1-4.3. In Fig. 4.3(a),  $v_{s,n}$  is reduced to 120 V, while the other phases are at the nominal value of 220 V. By increasing the value of  $\beta$ ,  $V_{d,a}$  is established by the DVR and  $V_{o,a}$  can be kept at 220 V. Thus, part of the energy supplied to phase-a load is supported by phase's b and c.

In Fig. 4.3(b), all three phases are unbalanced, where  $V_{s,a} = 210$  V,  $V_{s,b} = 190$  V, and  $V_{s,c} = 240$  V. Again, by adjusting the value of  $\beta$ ,  $V_{o,a}$ ,  $V_{o,b}$ , and  $V_{o,c}$  are regulated at 220 V. For the phase transformation between  $\beta$  and  $\theta_n$

$$\alpha = -(\beta - \phi_n - \theta_n) \quad \dots 4.23$$

Where  $\alpha_n$  is the phase difference between

$V_{s,n}$  and  $V_{d,n}$ .

Based on Fig. 4.3(a) and by using Equations (4.19) to (4.23), it can be shown that the steady-state power-transfer equation can be expressed as follows:

$$P_n = i_{o,n} \sqrt{v_{o,n}^2 + v_{s,n}^2 - 2v_{o,n}v_{s,n} \cos \beta} \times \cos \left[ \beta - \theta_n + \cos^{-1} \left( \frac{v_{s,n} - v_{o,n} \cos \beta}{\sqrt{v_{o,n}^2 + v_{s,n}^2 - 2v_{o,n}v_{s,n} \cos \beta}} \right) \right] \quad \dots 4.24$$

Detailed derivation of (34) is given in the Appendix. The values of  $v_{s,n}$ ,  $v_{o,n}$ ,  $i_{o,n}$ , and  $\theta_n$  are different in each phase. Thus, the power flow of each phase inverter is different.  $\beta$  is controlled by the outer loop in order to achieve power equilibrium in the system, and thus, satisfy eq.4.16 and 4.17.

TABLE 4.1 SPECIFICATIONS OF THE DVR

Parameters	Minimum	Nominal	Maximum
Supply voltage, $v_{s,n}$	110V	220V	280V
Load voltage, $v_{o,n}$	~	220V	~
Output current, $i_{o,n}$	0.1A	~	4A
Power factor, $\cos \theta_n$	0	~	0.996
dc link voltage, $v_{dc}$	200V	380V	450V
$v_{LD}$		2V	
$I_{ripple}$		2.6A	
Switching frequency		15kHz	

TABLE 4.2 PARAMETERS OF THE PLL AND TRANSDUCER GAINS

Parameter	Value	Parameter	Value
$V_{cc}$	5V	$K_{pid}$	1.59
$\beta_{max}$	0.785rad	$K_{vco}$	150
$V_{\beta,max}$	2.5V	$f_{LP}$	16Hz
$K_{T1}$	1/80		

TABLE 4.3 COMPONENT VALUES OF THE DVR

Parameter	Value	Parameter	Value
$L$	1mH	$C$	9.4F
$R_1$	30k	$C_1$	22F
$R_2$	300k	$C_2$	2.2F
$R_l$	10k	$C_l$	2.2F
$R_c$	20k	$C_{dc}$	1.36mF

### B. Small Signal Modeling

Fig. 4.5 shows the small-signal model of the outer loop. It consists of the transfer characteristics of the inner loop, inverter, PLL, and power-flow controller. As the inner loop has much faster dynamic response than the outer loop, the small-signal transfer function of the inner loop is unity. The transfer function of the inverter describes the small-signal behaviors between  $\beta$  and  $V_{dc}$ . The functional blocks of power stage and controller are derived as follows.

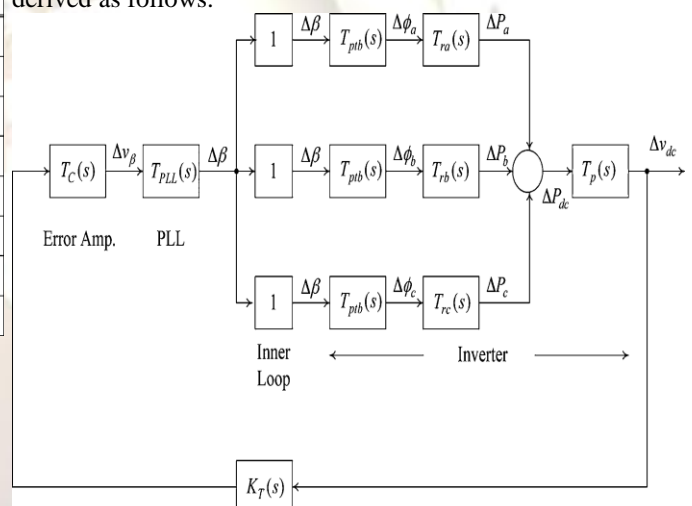


Fig.4.5. Small-signal model of the outer loop

1) Relationship Between  $V_{dc}$  and  $P_{dc}$ : The small-signal dclink voltage to dc-power-transfer function  $T_p(s)$  is as follows:

$$T_p(s) = \frac{\Delta v_{dc}(s)}{\Delta p_{dc}(s)} = \frac{2}{s c_{dc} v_{dc}} \quad \dots 4.25$$

Where  $V_{dc}$  is the steady-state values of  $V_{dc}$ .

2) Relationship between Power Flow and the Phase of  $V_d$  With Respect to  $i_{o,n}$  in Each Phase: The small-signal DVR phase- to-power transfer function  $T_{r,n}(s)$

$$T_{r,n}(s) = \left[ \frac{\Delta p_n(s)}{\Delta \phi_n(s)} \right] = -v_{d,n} i_{o,n} \quad \dots 4.26$$

Where  $V_d$  is the steady-state values of  $v_d$ .

3) Phase Transformation Between  $\beta$  and  $\phi$  in Each Phase: The transfer function  $T_{pt,n}(s)$  representing the transformation between  $\beta$  and  $\phi$  is

$$T_{pt,n} = \left[ \frac{\Delta \phi_n}{\Delta \beta_n} \right] = \frac{v_{s,n}}{v_{d,n}} \frac{v_{s,n} - v_{o,n} \cos \beta}{\sqrt{v_{o,n}^2 + v_{s,n}^2 - 2v_{o,n}v_{s,n} \cos \beta}} \quad \dots 4.27$$

Where  $V_s$ ,  $V_o$ , and  $B$  are the steady-state values of  $v_s$ ,  $v_o$ , and  $\beta$ , respectively.

4) Phase Transformation Between  $\beta$  and  $v_{dc}$  in Inverter: The transfer function  $T_{inv}(s)$  of the inverter is as follows [19]–[22]:

$$T_{inv} = \left[ \frac{\Delta v_{dc}(s)}{\Delta \beta(s)} \right] = -\frac{2}{sC_d v_{dc}} (v_{s,a} i_{o,a} \cos \alpha_a + v_{s,b} i_{o,b} \cos \alpha_b + v_{s,c} i_{o,c} \cos \alpha_c) \quad \dots 4.28$$

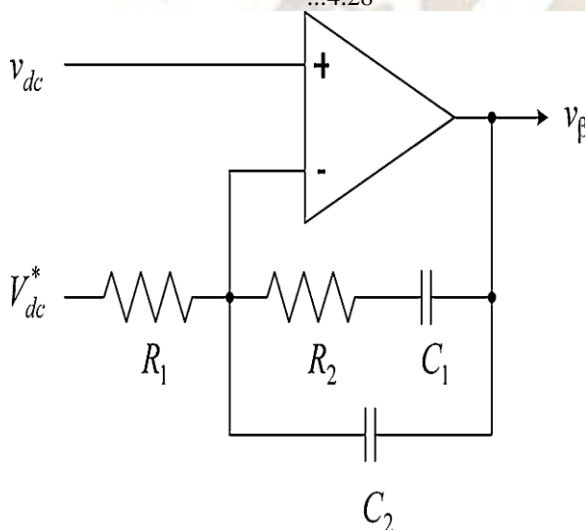


Fig.4.6. Circuit schematic of the power-flow controller

5) PLL: The PLL consists of three components, including the phase detector (PD), loop filter (LF), and the voltage controlled oscillator (VCO) [27]. Based on the small-signal model of the PLL is as follows:

$$T_{PLL}(s) = \frac{\Delta \beta(s)}{\Delta v_{\beta}(s)} = \frac{T_{VCO}(s)F_C(s)}{1 - T_{VCO}(s)T_{pd}(s)F_L(s)} = A \frac{\omega_n^2}{s^2 + 2\xi\omega_n s + \omega_n^2} \quad \dots 4.29$$

Where  $A = - (R_1 / (R_c K_{pd}))$ ;  $\xi = 0.5 \sqrt{\tau K_{pd} K_1 K_{vco}}$ ;  $\omega_n = \sqrt{(K_{pd} K_1 K_{vco} / T)}$  ...4.30

$K_{pd}, K_1, K_{vco}$  are the constant gains of PD, LF and VCO, respectively.

1. Power-Flow Controller:

The function of the power-flow controller is to regulate  $v_{dc}$  at the reference voltage  $V_{dc}$ , which is determined by the voltage ratings of the capacitor and the switches. Charging or discharging the capacitor  $C_{dc}$  is achieved by adjusting  $\phi_n$  in three phases individually. The regulation action is performed by the error amplifier shown in Fig. 4.6. The transfer function  $TC(s)$  can be shown in (Eq.4.29-4.30), at the bottom of the page.

#### 4.4. SIMPLIFIED DESIGN PROCEDURES:

The values of  $L$ ,  $C$ , and  $C_{dc}$  in the inverter,  $R_1$ ,  $R_2$ ,  $C_1$ , and  $C_2$  in the power-flow controller are designed as follows.

A. Design of  $L$  and  $C$  in the Inverter:

The values of  $L$  and  $C$  in the output filters are determined by considering the maximum voltage drop across the inductor  $v_L$ ,  $D$  at the maximum line current  $I_{o,max}$ , angular line frequency  $\omega$ , maximum ripple current  $I_{ripple}$ , and angular switching frequency  $\omega_{sw}$ . As most of the load current is designed to flow through  $L$ , the value of  $L$  is determined by considering that its voltage drop  $v_L$ ,  $D$  is small at the maximum line current  $I_{o,max}$ .

Thus

$$\omega L I_{o,max} < v_{L,D} = L < (v_{L,D} / \omega I_{o,max}) \quad \dots 4.31a$$

As the inverter output consists of high-frequency harmonics, the fundamental component of the ripple current through the filter is designed to be less than  $I_{ripple}$ . For the sake of simplicity in the calculation, the load impedance at the switching frequency is assumed to be infinite.

Thus

$$\frac{2v_{dc}}{\pi} \frac{1}{\omega_{sw} L - \left( \frac{1}{\omega_{sw} C} \right)} < I_{ripple} \text{ \& } C > \frac{1}{\omega_{sw} \left( \omega_{sw} L - \left( \frac{2v_{dc}}{\pi I_{ripple}} \right) \right)} \quad \dots 4.31(b)$$

The nominal switching frequency is chosen to be a few hundred times the line frequency.  $v_{L,D}$  is chosen to be 1% of the line voltage, and  $I_{ripple}$  is chosen to be one half of the peak of the line current. As shown in Table I,  $\omega_{sw} = 300 \omega$ ,  $v_{L,D} = 2$  V, and  $I_{ripple} = 2.6$  A for the designed prototype. Based on (Eq.4.31) and stated criteria, the values of  $L$  and  $C$  in the output filters are determined.

B. Design of  $C_{dc}$  in the Inverter:

The value of  $C_{dc}$  is determined by

$$C_{dc} = \frac{4(v_{o,nor} - v_{s,min})(i_{o,a} \cos \theta_a + i_{o,b} \cos \theta_b + i_{o,c} \cos \theta_c)t_{res}}{v_{dc,ref}^2 - 8(v_{o,nor} - v_{s,min})^2} \dots 4.32$$

Where vo, nor and vs, min are nominal value of load voltage and minimum voltage of supply voltage in specification, respectively, tres is duration of restoration.

C. Design of R1 , R2 , C1 , and C2 in the Power-Flow Controller:

The pole and zeros are designed as follows:

$$\log \omega_p = \text{Log } \omega_{z2} - (\psi/20) \dots 4.33$$

Typically,  $\psi = 20$  is chosen, and the ratio of  $\omega_{z1}$  and  $\omega_{z2}$  is chosen to be at least 100, in order to avoid overlapping in the two zeros.

$$\Rightarrow \log \omega_z = \log \omega_z^2 - 2 \dots 4.34$$

Based on Eq. (4.35)–(4.37), R1 , R2 , C1 , and C2 are designed by putting a value into one of them. The practical simulation model of DVR is shown in Fig 4.9. The loop gain TOL(s), it is based on the specifications and designed component values listed in Tables 4.2 and 4.3. The bode plot shows operation range, the frequency between  $\omega_{cross, min}$  and  $\omega_{cross, max}$  within the stable regions. Based on Eq. (4.30), we have

$$\omega_{z1} + \omega_{z1} = (1/R_2 C_2) + (1/R_2 C_1) + (1/R_1 C_2) \dots 4.35$$

$$\omega_{z1} * \omega_{z1} = (1/R_1 R_2 C_1 e C_2) \dots 4.36$$

$$\omega_p = (C_1 + C_2)/(C_1 C_2 R_1) \dots 4.37$$

#### 4.5 RESULT ANALYSIS OF A FAST DYNAMIC CONTROL SCHEME FOR CAPACITOR-SUPPORTED INTERLINE DYNAMIC VOLTAGE RESTORER

##### 4.5.1. Harmonic Distortions:

When large amount of loads are added or removed at the load centre's a dip in voltage level will take place and that can abrupt performance of the customer's equipment. The above mentioned are two major power quality issues that existing in the power systems. Due these effects the total harmonic distortion that is transmitted in the line is 33.54% for one complete cycle of the waveform and the transmitted signals will affect the performance of the line as shown in the fig.4.7.

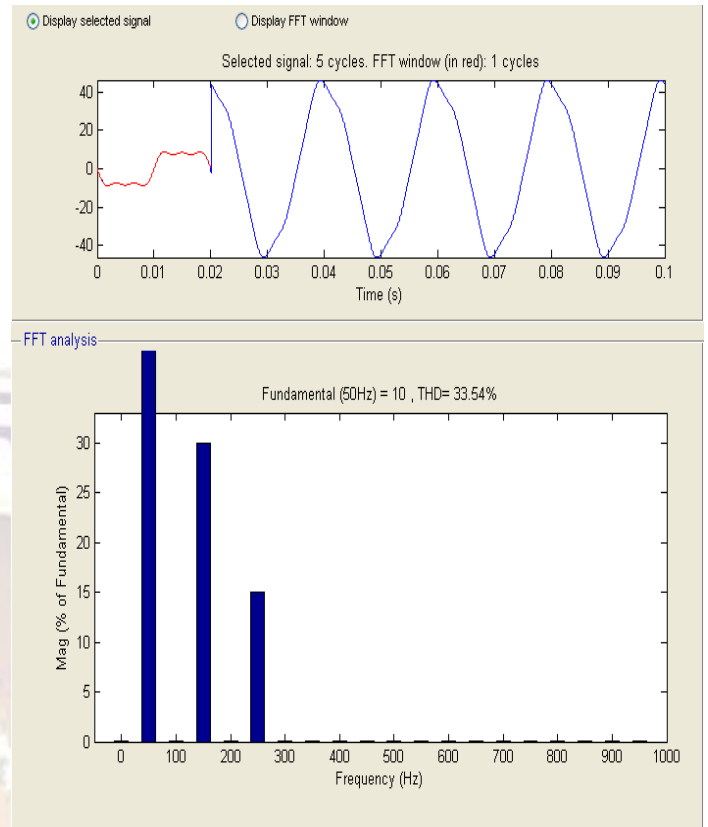


Fig. 4.7 The voltage and harmonic analysis of waveform without DVR

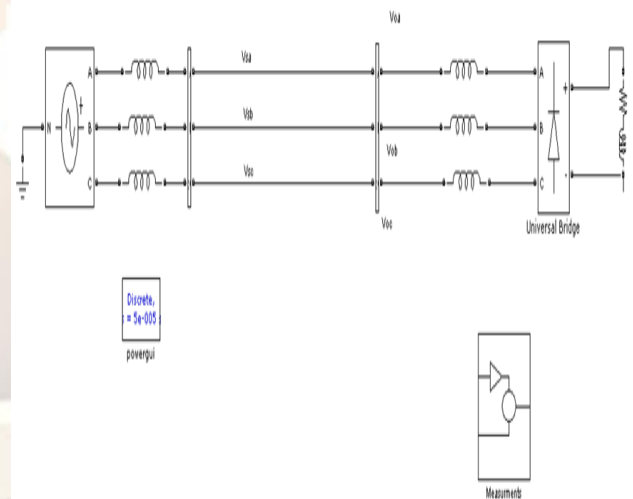


Fig.4.8 Simulation model without DVR

When large amount of loads are connected the dip in voltage will rise which can be reduced by using a dynamic voltage restorer. The sag that is reduced by using the DVR is shown in the below fig.4.9. The storage element in the DVR i.e. capacitor stored energy will be used to bounce back the sagged phases to nominal values and the total harmonic distortion can be reduce to 1.37% from a value 33.54% as shown in fig 4.9.

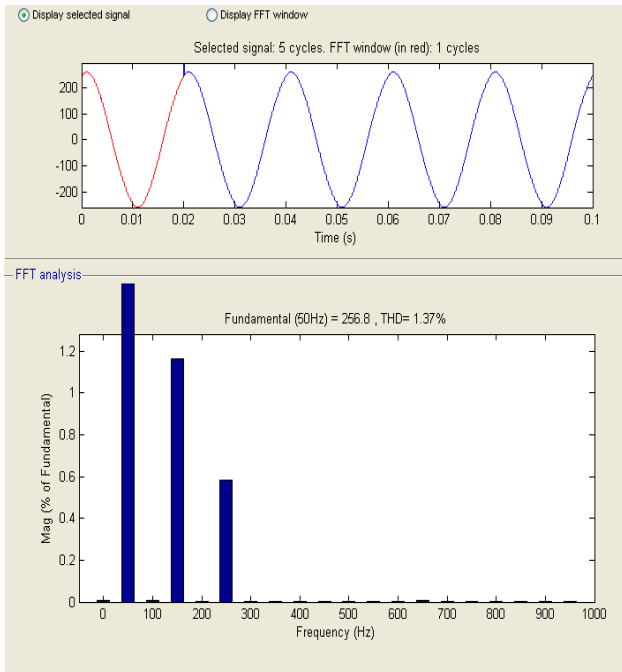


Fig.4.9 The voltage and harmonic analysis of waveform with DVR

The voltage sag and swell cases that are compensated by the dynamic voltage restorer are shown in the fig. (4.11)

#### 4.5.1. Voltage Sag:

The voltage sag effected on single and three phase conditions are shown in the fig.4.11 where the supply voltage is reduced from a value of  $V_s=220V$  rms to  $120V$  rms i.e. the percentage of sag that resulted is around 45%. When a sag occurs in the voltage then outer control loop and inner control loop will initiate to release the energy stored in the capacitor to restore the supply voltage to nominal value. The voltage sag is compensated with the transition time  $250\mu\text{sec}$  to  $180\mu\text{sec}$ .

#### 4.5.2. Voltage Swell:

The voltage swell effected on single and three phase conditions are shown in the fig.4.11 where the supply voltage is increased from a value of  $V_s=220V$  rms to  $260V$  rms i.e. the percentage of swell that resulted is around 19%. When a voltage swell occurs in the voltage then outer control loop and inner control loop will initiate to charge the capacitor to restore the supply voltage to nominal value. The voltage swell is compensated with the transition time of  $180\mu\text{sec}$ . The dynamic voltage restorer provides the compensation to the harmonics contents, voltage sag and voltage swell cases.

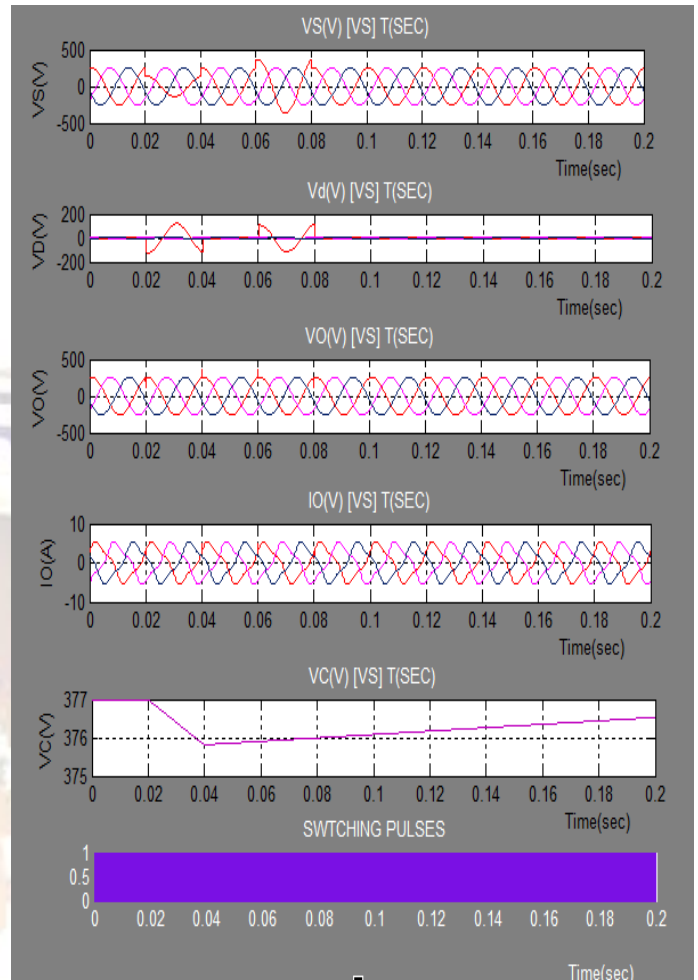


Fig.4.11 Waveforms at three sagged and swelled phases under condition.  $V_{s,a}$ ,  $V_{s,b}$ , and  $V_{s,c}$  are changed from  $220V$  to  $120V_{rms}$  and  $220V$  to  $260V$ .

#### 4.6. COMPARISON OF RESULTS WITH AND WITHOUT DVR:

The effect of voltage sag and swell has a greater impact on the power that is transmitted from sending end to receiving end. The real power that is transmitted gets varied due to the addition of more non-linear loads or sudden shutdown of large rating loads. The voltage sag and swell cases cause customer appliances to get abrupt by reducing their life span. The power quality at the load centre are mostly electronic switched ones, so due to the switching actions of these non-linear loads the level of harmonics injected into the supply will be more and the cost of the capacitors required to compensate the harmonics will increase there by increasing the overall cost.

When an automatically controlled regulators are used then the chances of overcoming the voltage sag or swell cases can be avoided. The dynamic voltage restorer operates at desired levels to regulate voltages as well as eliminates the harmonics. The entire mechanism uses capacitor banks to restore the voltage to nominal values and

the energy stored in the capacitor can be charged from the supply it self. Under normal operated conditions the MOSFET switches which operate at 10 KHz frequency nor inject nor charge the capacitor. When a voltage sag occur the stored energy restores the voltage to nominal value by discharging the energy. When a voltage swell occur in any of the phases, the capacitor uses the swelled phase to charge its energy to bounce to normal full capacity.

The total harmonic content that will be available when a power system is operated under sagged condition will be 33.54% i.e without using the DVR. When a DVR is used in to back up the sagged voltage to nominal value it also eliminates the total harmonic content to a lower value less than 6%.

## V. CONCLUSION

A control scheme for three-phase capacitor-supported interline DVR has been presented. By integrating a recently proposed boundary-control method with second-order switching surface (inner loop), the dynamic response has been minimized to two switching actions. The voltage sag, swell, and voltage harmonic distortion have been compensated by this DVR. Moreover, by using series bidirectional inverter as DVR, capacitor banks are used to support the dc link and the sagged phase(s) could be supported by the un sagged phase(s). Long-duration voltage sags and swell and three-phase voltage unbalance could be overcome by the proposed power-flow controller (outer loop). The MOSFET switches that are used in the voltage source converter operate at a variable frequency range i.e. 10 KHz. This has facilitated for the fast switching action and provides dynamic response in turn maintains the stability of the system. The designed model of dynamic voltage restorer also reduces the harmonic percentages that resulted due to MOSFET switching actions. The gating pulse to the switch is generated by the pulse width modulation technique. The method has been verified with a review model. The performances of the DVR have been demonstrated and evaluated with different power-quality disturbances. Experimental measurements are favorably verified with theoretical results. The power quality problem issues related to voltage sag and swell as well as total harmonic distortion can be compensated effectively by using the dynamic voltage restorer.

## REFERENCES

- [1] M. Bollen, Understanding Power Quality Problems, Voltage Sags and Interruptions. New York: IEEE Press, 2000.
- [2] M. Sullivan, T. Vardell, and M. Johnson, "Power interruption costs to industrial and

- commercial consumers of electricity," *IEEE Trans. Ind. App.*, vol. 33, no. 6, pp. 1448–1458, Nov. 1997.
- [3] N. Woodley, L. Morgan, and A. Sundaram, "Experience with an inverter based dynamic voltage restorer," *IEEE Trans. Power Del.*, vol. 14, no. 3, pp. 1181–1186, Jul. 1999.
- [4] R. R. Erra belli, Y. Y. Kolhatkar, and S. P. Das, "Experimental investigation of DVR with sliding mode control," in *Proc. IEEE Power India Conf.*, Apr. 2006, paper 117.
- [5] S. Lee, H. Kim, and S. K. Sul, "A novel control method for the compensation voltages in dynamic voltage restorers," in *Proc. IEEE APEC 2004*, vol. 1, pp. 614–620.
- [6] G. Joos, S. Chen, and L. Lopes, "Closed-loop state variable control of dynamic voltage restorers with fast compensation characteristics," in *Proc. IEEE IAS 2004*, Oct., vol. 4, pp. 2252–2258.
- [7] P. Ruilin and Z. Yuegen, "Sliding mode control strategy of dynamic voltage restorer," in *Proc. ICIECA 2005*, Nov./Dec., p. 3.
- [8] T. Jauch, A. Kara, M. Rahmani, and D. Westermann, "Power quality ensured by dynamic voltage correction," *ABB Rev.*, vol. 4, 1998, pp. 25–36.
- [9] C.S. Chang, S.W. Yang, and Y. S. Ho, "Simulation and analysis of series voltage restorer (SVR) for voltage sag relief," in *Proc. IEEE PES Winter Meeting*, Jan, 2000, vol. 4, pp. 2476–2481.
- [10] C. Meyer, R. W. De Doncker, Y. W. Li, and F. Blaabjerg, "Optimized control strategy for a medium-voltage DVR—Theoretical investigations and experimental results," *IEEE Trans. Power Electron.*, vol. 23, no. 6, pp. 2746–2754, Nov. 2008.
- [11] S. S. Choi, B. H. Li, and D. M. Vilathgamuwa, "Dynamic voltage regulation with minimum energy injection," *IEEE Trans. Power Syst.*, vol. 15, no. 1, pp. 51–57, Feb. 2000.
- [12] D. M. Vilathgamuwa, A. A. D. R. Perera, and S. S. Choi, "Voltage sag compensation with energy optimized dynamic voltage restorer," *IEEE Trans. Power Del.*, vol. 18, no. 3, pp. 928–936, Jul. 2003.
- [13] K. Piatek, "A new approach of DVR control with minimized energy injection," in *Proc. PEMC2006*, Aug., pp. 1490–1495.
- [14] D. M. Vilathgamuwa, H.M.Wijekoon, and S. S. Choi, "Interline dynamic voltage restorer: A novel and economical approach for multilines power quality compensation,"

- IEEE Trans. Ind. Appl.*, vol. 40, no. 6, pp. 1678–1685, Nov./Dec. 2004.
- [15] D. Vilathgamuwa, H.M.Wijekoon, and S. S. Choi, “A novel technique to compensate voltage sags in multiline distribution system—The interline dynamic voltage restorer,” *IEEE Trans. Ind. Electron.*, vol. 53, no. 5, pp. 1603–1611, Oct. 2006.
- [16] R. J. Nelson and D. G. Ramey, “Dynamic power and voltage regulator for an ac transmission line,” U.S. Patent 5 610 501, Mar. 1997. [17] A. van Zyl, R. Spee, A. Faveluke, and S. Bhowmik, “Voltage sag ride-through for adjustable-speed drives with active rectifiers,” *IEEE Trans. Ind. Appl.*, vol. 34, no. 6, pp. 1270–1277, Nov./Dec. 1998.
- [18] A. Ghosh, A. K. Jindal, and A. Joshi, “Design of a capacitor-supported dynamic voltage restorer (DVR) for unbalanced and distorted loads,” *IEEE Trans. Power Del.*, vol. 19, no. 1, pp. 405–413, Jan. 2004.
- [19] C. Ho, H. Chung, and K. Au, “Design and implementation of a fast dynamic control scheme for capacitor-supported dynamic voltage restorers,” *IEEE Trans. Power Electron.*, vol. 23, no. 1, pp. 237–251, Jan. 2008.
- [20] K. Leung and H. Chung, “Derivation of a second-order switching surface in the boundary control of buck converters,” *IEEE Power Electron. Lett.*, vol. 2, no. 2, pp. 63–67, Jun. 2004.
- [21] K. Leung and H. Chung, “A comparative study of the boundary control of buck converters using first- and second-order switching surfaces,” *IEEE Trans. Power Electron.*, vol. 22, no. 4, pp. 1196–1209, Jul. 2007.
- [22] D. O. Koval and M. B. Hughes, “Canadian national power quality survey: Frequency of industrial and commercial voltage sags,” *IEEE Trans. Ind. Appl.*, vol. 33, no. 3, pp. 622–627, May/Jun. 1997.
- [23] A. El Mofty and K. Youssef, “Industrial power quality problems,” in *Proc. IEE Conf. Electr. Distrib., Part 1: Contrib.*, Jun. 2001, vol. 2, pp. 139–139.
- [24] E. W. Gunther and H. Mehta, “A survey of distribution system power quality—Preliminary results,” *IEEE Trans. Power Del.*, vol. 10, no. 1, pp. 322–329, Jan. 1995.
- [25] M. H. J. Bollen, “Voltage sags: Effects, mitigation and prediction,” *Power Eng. J.*, vol. 10, no. 3, pp. 129–135, Jun. 1996.
- [26] B. M. Weedy and B. J. Cory, *Electric Power System*, 4th ed. New York: Wiley, 1998.
- [27] H. M. Berlin, *Design of Phase-Locked Loop Circuits with Experiments*, 1st ed. Indianapolis, IN: Sams, 1985.
- [28] H. Kim and S. K. Sul, “Compensation voltage control in dynamic voltage restorers by use of feed forward and state feedback scheme,” *IEEE Trans. Power Electron.*, vol. 20, no. 5, pp. 1169–1176, Jan. 2005.
- [29] B. Wang, G. Venkataramanan, and M. Illindala, “Operation and control of a dynamic voltage restorer using transformer coupled H-bridge converters,” *IEEE Trans. Power Electron.*, vol. 21, no. 4, pp. 1053–1061, Jun. 2006.
- [30] H. Awad, J. Svensson, and M. Bollen, “Mitigation of unbalanced voltage dips using static series compensator,” *IEEE Trans. Power Electron.*, vol. 19, no. 3, pp. 837–846, May 2004.
- [31] Y. Chiu, K. Leung, and H. Chung, “High-order switching surface in boundary control of inverters,” *IEEE Trans. Power Electron.*, vol. 22, no. 5, pp. 1753–1765, Sep. 2007.
- [32] M. Ordonez, J. E. Quaiçoe, and M. T. Iqbal, “Advanced boundary control of inverters using the natural switching surface: Normalized geometrical derivation,” *IEEE Trans. Power Electron.*, vol. 23, no. 6, pp. 2915–2930, Nov. 2008.
- [33] S. Chen, Y. M. Lai, S. C. Tan, and C. K. Tse, “Boundary control with ripple-derived switching surface for DC–AC inverters,” *IEEE Trans. Power Electron.*, vol. 24, no. 12, pp. 2873–2885, Dec. 2009.
- [34] M. Rashid, *Power Electronics, Circuits, Devices, and Applications*, 3<sup>rd</sup> ed. Englewood Cliffs, NJ: Prentice-Hall, 2004.]
- [35] C. Ho, K. Au, and H. Chung, “Digital implementation of boundary control with second-order switching surface,” in *Proc. IEEE PESC2007*, Jun., pp. 1658–1664 applications and extensions.